Brain Stimulation 11 (2018) 727–733

Contents lists available at ScienceDirect

Brain Stimulation

journal homepage: http://www.journals.elsevier.com/brain-stimulation

Evidence of transcranial direct current stimulation-generated electric fields at subthalamic level in human brain *in vivo*

Pratik Y. Chhatbar [a], Steven A. Kautz [b, c], Istvan Takacs [d], Nathan C. Rowland [d], Gonzalo J. Revuelta [a], Mark S. George [c, e], Marom Bikson [f], Wuwei Feng [a, b, *]

[a] Department of Neurology, College of Medicine, Medical University of South Carolina, Charleston, SC, USA
[b] Department of Health Science & Research, College of Health Professions, Medical University of South Carolina, Charleston, SC, USA
[c] Ralph H. Johnson VA Medical Center, Charleston, SC, USA
[d] Department of Neurosurgery, College of Medicine, Medical University of South Carolina, Charleston, SC, USA
[e] Brain Stimulation Laboratory, Department of Psychiatry and Behavioral Science, College of Medicine, Medical University of South Carolina, Charleston, SC, USA
[f] Department of Biomedical Engineering, The City College of The City University of New York, New York, NY, USA

ARTICLE INFO

Article history:
Received 22 December 2017
Received in revised form
28 February 2018
Accepted 8 March 2018
Available online 13 March 2018

Keywords:
Deep brain stimulation
Transcranial direct current stimulation
Body resistance
Dose-dependence
Voltage-current relationship

ABSTRACT

Background: Transcranial direct current stimulation (tDCS) is a promising brain modulation technique for several disease conditions. With this technique, some portion of the current penetrates through the scalp to the cortex and modulates cortical excitability, but a recent human cadaver study questions the amount. This insufficient intracerebral penetration of currents may partially explain the inconsistent and mixed results in tDCS studies to date. Experimental validation of a transcranial alternating current stimulation-generated electric field (EF) *in vivo* has been performed on the cortical (using electrocorticography, ECoG, electrodes), subcortical (using stereo electroencephalography, SEEG, electrodes) and deeper thalamic/subthalamic levels (using DBS electrodes). However, tDCS-generated EF measurements have never been attempted.

Objective: We aimed to demonstrate that tDCS generates biologically relevant EF as deep as the subthalamic level *in vivo*.

Methods: Patients with movement disorders who have implanted deep brain stimulation (DBS) electrodes serve as a natural experimental model for thalamic/subthalamic recordings of tDCS-generated EF. We measured voltage changes from DBS electrodes and body resistance from tDCS electrodes in three subjects while applying direct current to the scalp at 2 mA and 4 mA over two tDCS montages.

Results: Voltage changes at the level of deep nuclei changed proportionally with the level of applied current and varied with different tDCS montages.

Conclusions: Our findings suggest that scalp-applied tDCS generates biologically relevant EF. Incorporation of these experimental results may improve finite element analysis (FEA)-based models.

Introduction

Transcranial direct current stimulation (tDCS) can modulate brain activity and induce behavioral changes, showing promise for treating several disease conditions [1]. However, concerns have been raised that the majority of the applied current shunts at the level of the scalp [2], implying that only a potentially trivial amount of current penetrates the brain with existing human tDCS protocols (up to 2 mA of applied current). Although finite element analysis (FEA)-based simulation models predict the presence of tDCS generated electric fields (EF) throughout the brain [3], there is no direct evidence demonstrating or quanitfying this in the deep areas of the living human brain. In this experiment, we aimed to detect and measure tDCS-generated voltage changes using implanted DBS electrodes in patients with movement disorders. These patients serve as natural models and allow us to address this critical research question.

Materials and methods

The Institutional Review Board at the Medical University of South Carolina approved all procedures, and all subjects signed

* Corresponding author. Department of Neurology, Medical University of South Carolina, 19 Hagood Ave, Suite 501, Charleston, SC 29425, USA.
E-mail addresses: feng@musc.edu, cnwwfeng@rocketmail.com (W. Feng).

https://doi.org/10.1016/j.brs.2018.03.006
1935-861X/

written consents. Our targeted population was subjects with implanted deep brain stimulation (DBS) electrode(s) (stage I procedure). For our experiment, they were scheduled for installment/replacement of an implantable pulse generator (IPG, stage II procedure). The detailed inclusion and exclusion criteria are included in Table 1. The experiment was conducted in the operating room. The research protocol was integrated with the clinical care protocol so that it did not interrupt clinical care (Fig. 1). Detailed procedure steps are listed in the Supplementary material.

tDCS protocol

We applied tDCS with an iontophoresis device (Chattanooga Group, Hixson, TN) connected to biocarbon electrodes embedded in a 5×7 cm^2 sponge pad (Soterix Medical, New York, NY). We tested current strengths of 2 mA or 4 mA first under bitemporal (anode on the left temple, cathode on the right temple), followed by occipitofrontal (anode over the occipital bone, cathode over the forehead) montages. The selection and order of montage and tDCS current strengths were varied across the subjects. Single stimulation trials were 3 min, including ramp-up and ramp-down times. We monitored the applied voltage and injected currents using DI-245 data acquisition (DAQ) device (DATAQ Instruments, Inc., Akron, OH) throughout stimulation at 50 Hz. DI-245 has an input impedance of 1 MΩ, a common mode rejection of 110 dB, and a 14-bit resolution. We used $1\times$ gain for applied voltage measurements between the anode and cathode, allowing us the range of ±50 V (6.1 mV/bit resolution). For current measurements, we measured the voltage across a 250 Ω resistor installed in series between the tDCS device and the tDCS electrode with $20\times$ gain (±2.5 V, 0.3 mV/bit resolution). Per Ohm's law, this allowed us to measure up to ±10 mA (1.22 μA/bit resolution) of current. We also calculated body resistance as a ratio of applied voltage and injected current using Ohm's law.

Electric field (EF) recording protocol

We measured the EF inside the brain using the implanted DBS electrode(s). In the sterile operative field, the neurosurgeon connected the DBS lead terminals with the trialing cable connector (Part 355531, Medtronic, Inc., Minneapolis, MN), and passed the other end to be connected with the recording setup in the non-sterile area. Using a custom connector, we recorded EF using DI-710-UL data acquisition (DAQ) device (DATAQ Instruments, Inc., Akron, OH) throughout stimulation at 50 Hz. DI-710-UL has an input impedance of 1 MΩ, common mode rejection of 80 dB, and 14-bit resolution. We recorded EF at $100\times$ gain, allowing the recordings to be in the range of ±100 mV and resolution of 12.21 μV/bit. For the subject with a unilateral DBS lead, the reference electrode for recording was positioned extracranially on the chest wall. For the subjects with bilateral DBS, the reference electrode was one of the DBS electrodes. Since we wanted to record the tDCS-generated EF, we did not use any band-pass filtering to ensure that the characteristic DC pattern does not get filtered out. The trade-off for not using band-pass filtering was the introduction of DC bias (constant voltage change as a result of lack of high-pass filtering) and DC drift (slew, or slow change in DC voltage change over time) in the recordings.

Table 1
Study selection criteria.

Inclusion criteria (meet ALL)	Exclusion criteria (meet ANY)
- Adult patients (18 + years) of any race, who are already scheduled to have surgical DBS procedure as part of clinical care determined by DBS program - Capable and willing to give consent (Legally Authorized Representative is not allowed for this study) - Availability of the brain MRI	- Documented severe depression or other neuropsychiatric disease(s) despite medications - Documented severe dementia (with or without medications) with Mini Mental Status Examination score <17 - Prior brain surgery (except stage I procedure); - Severe scalp/skin disease (including but not limit to purpura, blisters, rash, eczema) or open wound/laceration; - Presence of known tDCS risk factors, e.g., a) an electrically, magnetically or mechanically activated metal or nonmetal implant including cardiac pacemaker, intracerebral vascular clips or any other electrically sensitive support system; b) non-fixed metal in any part of the body, including a previous metallic injury to eye; c) pregnancy, since the effect of tDCS on the fetus is unknown; d) history of seizure disorder; e) preexisting scalp lesion that can interfere with tDCS pad application;

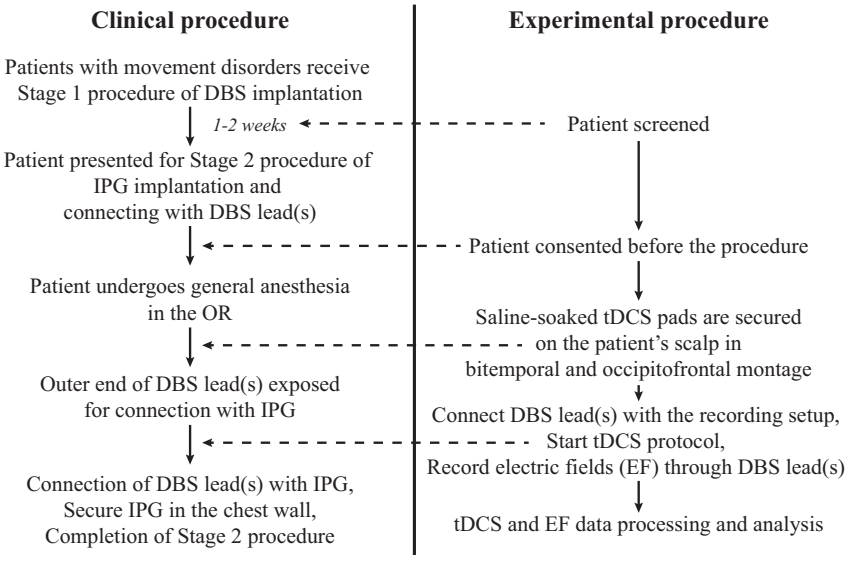

Fig. 1. An overview of the clinical procedure interspersed with the experimental procedure.

Data analysis

To minimize DC bias and DC drift (see above), we demeaned (by subtracting average voltage value) and detrended (by correcting for the slope of voltage) individual sections of tDCS-on and tDCS-off recordings on each DBS electrode. The tDCS-on section was defined as injected tDCS current higher than the predefined noise floor (we used 5 μA as the noise floor). The tDCS-off section was without injected tDCS current (<5 μA). Both the tDCS-on and tDCS-off sections were conditioned in exactly the same way. For the data analysis and comparison of the magnitude of voltage change and body resistance, we used the values at the time of initiation of tDCS ramp-down. We considered tDCS ramp-up as "completed" when the current intensity reached 95% of maximum current intensity. Peculiar to our tDCS hardware, the relatively low slope of the later ramp-up caused a significant duration of tDCS stimulation to be excluded as a "ramp-up" phase. By using 95% of maximum current intensity as our threshold, we sufficiently excluded the steep part of the ramp-up while allowing a mostly plateaued part of the ramp-up for the calculation of average voltage and resistance. The 95% cut-off allowed 1.9 mA and 3.8 mA to be considered as completed ramp-up for 2 mA and 4 mA stimulations, respectively. We calculated coefficients of determination (R^2) by using cross-correlation between voltage changes recorded at a given channel and values of injected tDCS current throughout the on or off section.

Results

We recruited three subjects who underwent the IPG installation or stage II procedure. Subject-specific characteristics are presented in Table 2. Injected current, body resistance and voltage difference at each electrode against the reference are shown in Fig. 2. Subject 1 had one 4-channel lead (Part 3387, Medtronic, Inc., Minneapolis, MN) implanted in the left ventrointermediate nucleus (VIM) for treating his essential tremor, and he was tested on the bitemporal tDCS montage at 2 mA only. We recorded voltage changes corresponding to an injected current of tDCS on all four electrodes of the leads with respect to the reference electrode positioned on the chest wall (Table 3; Fig. 2D). Differential recordings using electrode 2 on the DBS lead itself did not show appreciable voltage changes (Table 3; Fig. 2E), suggesting that EF orthogonal to the relative positions of DBS electrodes did not generate strong voltage changes across them. Both Subject 2 and 3 had two 4-channel leads (Part 3389, Medtronic, Inc., Minneapolis, MN). They were implanted in bilateral subthalamic nuclei (STN) for subject 2 and in bilateral internal globus pallidus (GPi) for subject 3 as the treatment for Parkinson's disease. The distance between the tips of the DBS leads was 2.36 cm for subject 2 and 4.35 cm for subject 3 (Table 2). Both the subjects were tested on the bitemporal montage followed by the occipitofrontal montage (Fig. 2G, I). We found that the bitemporal montage offered higher voltage differences across DBS leads. The occipitofrontal montage, however, offered relatively lower voltage differences across DBS leads (Table 3; Fig. 2G, I). Side by side positioning of DBS leads (coronal plane) resulted in such difference, because the general direction of EF in the bitemporal montage is in the coronal plane (Fig. 2A), while the general direction of EF in the occipitofrontal montage is in the sagittal plane (Fig. 2B). The magnitude of voltage changes corresponded to the amplitude of current under the bitemporal montage. In other words, current at 4 mA led to almost double the voltage changes across DBS electrodes when compared to the current at 2 mA under the bitemporal montage. For example, Channel 9 on subject 3 (inter-lead spacing of 4.35 cm, Table 2) showed an 11 mV voltage change on 4 mA tDCS, but 5.5 mV on 2 mA tDCS (Table 3). We also found that the body resistance was lower by about 20–30% during 4 mA stimulations versus the 2 mA stimulations in both bitemporal and occipitofrontal tDCS montages (Table 2, Fig. 2G, I). The order of stimulation strength did not appear to affect the body resistance.

Discussion

Scalp-applied tDCS can generate electrical fields deep inside the brain

To our knowledge, this is the first report in living humans of scalp tDCS-delivered voltage measurements across DBS electrodes at the level of subthalamic nuclei. Our findings demonstrate that scalp tDCS produces an EF deep inside the brain in a dose-dependent and montage-specific manner. Previous reports showed that transcranial alternating current stimulation (tACS) generated an EF at the cortical, subcortical and subthalamic levels using ECoG, SEEG and DBS electrodes, respectively [4–6]. However, the direct current-generated EF has not been reported to date. This is likely due to technical difficulties with the recording setup, which is typically designed for recording neural activity or local field potentials. For maximum amplification and minimum bias in the

Table 2
Subject characteristics.

Variables	Subject 1	Subject 2	Subject 3
Age/sex	77/M	60/M	71/M
Race	Caucasian	Caucasian	Caucasian
Head width (cm)	16.0	16.6	16.2
Head length (cm)	20.7	20.4	19.9
Head circumference (cm)	57.9	58.3	56.9
DBS indication	Essential tremor	Parkinson's disease	Parkinson's disease
Lead placement	Left ventro-intermediate nucleus (VIM)	Bilateral subthalamic nucleus (STN)	Bilateral internal globus pallidus (GPi)
Lead model	Medtronic 3387	Medtronic 3389	Medtronic 3389
Electrodes per lead	4	4	4
Inter-electrode spacing (center-to-center, mm)	3	2	2
Inter-lead spacing (cm)	N/A	2.36	4.35
Body resistance (kΩ)			
Bitemporal 2 mA	3.54	2.12	1.97
Bitemporal 4 mA	–	1.74	1.46
% Change during 4 mA as compared to 2 mA	-	−18.2%	−25.7%
Occipitofrontal 2 mA	–	1.90	2.51
Occipitofrontal 4 mA	–	1.34	1.95
% Change during 4 mA as compared to 2 mA	-	−29.5%	−22.2%

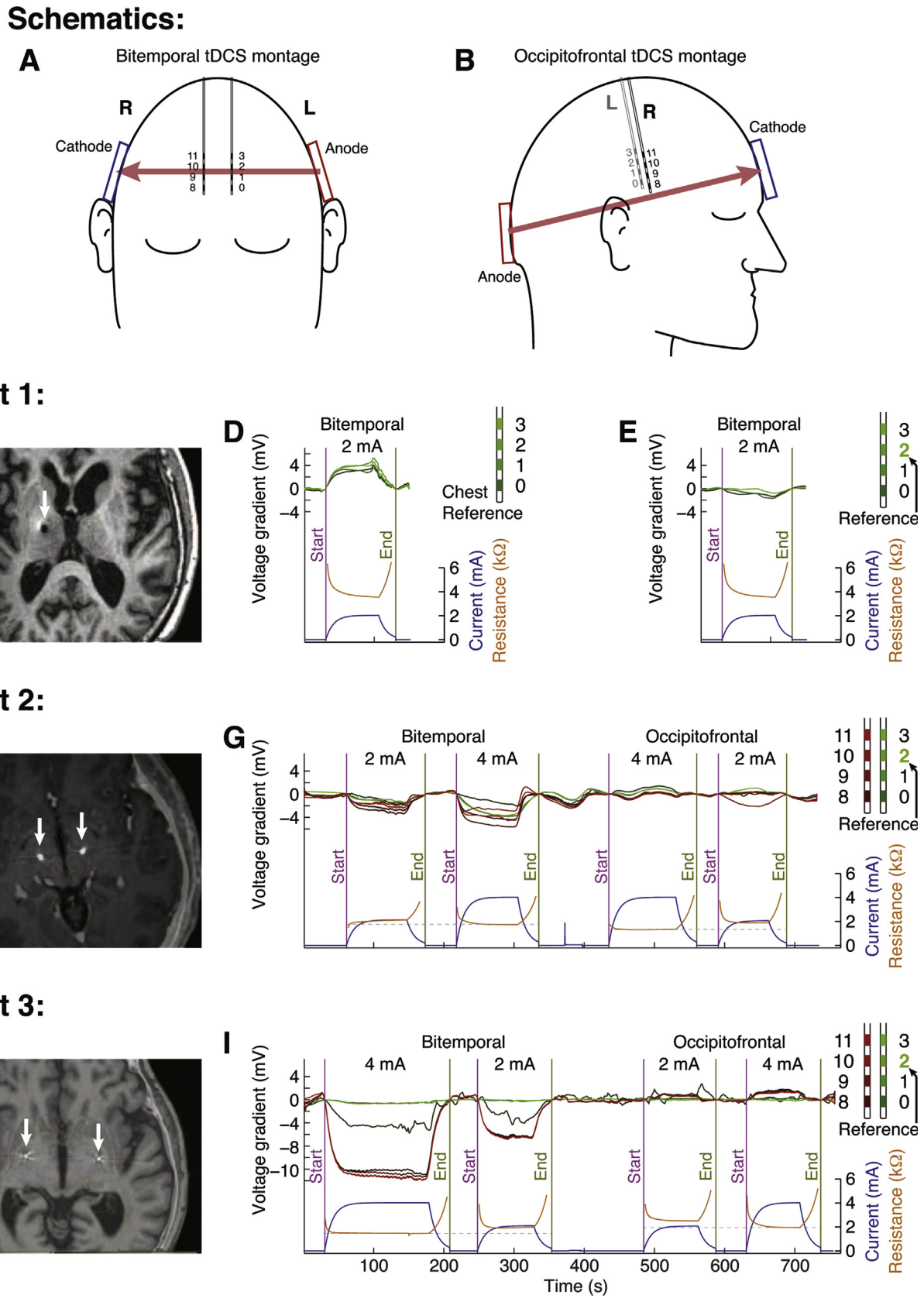
Schematics:
A
Bitemporal tDCS montage
R
L
Cathode
Anode
B
Occipitofrontal tDCS montage
L
R
Cathode
Anode
Subject 1:
C
D
Bitemporal
2 mA
Voltage gradient (mV)
Start
End
Chest
Reference
Current (mA)
Resistance (kΩ)
E
Bitemporal
2 mA
Reference
Subject 2:
F
G
Bitemporal
Occipitofrontal
2 mA
4 mA
4 mA
2 mA
Reference
Subject 3:
H
I
Bitemporal
Occipitofrontal
4 mA
2 mA
2 mA
4 mA
Time (s)

Table 3
Voltage changes and correlation (R^2) values of recorded voltage against injected tDCS currents.

tDCS section	On1	Off1	On2	Off2	On3	Off3	On4
Subject 1 (chest wall lead as a reference, Fig. 2D)							
	BT, 2 mA						
Channel 0	2.05 (0.94)	–	–	–	–	–	–
Channel 1	1.81 (0.90)	–	–	–	–	–	–
Channel 2	3.34 (0.95)	–	–	–	–	–	–
Channel 3	2.52 (0.95)	–	–	–	–	–	–
Subject 1 (Channel 2 as a reference, Fig. 2E)							
	BT, 2 mA						
Channel 0	−1.30 (0.78)	–	–	–	–	–	–
Channel 1	−1.53 (0.39)	–	–	–	–	–	–
Channel 3	−0.82 (0.05)	–	–	–	–	–	–
Subject 2 (Channel 2 as a reference, Fig. 2G)							
	BT, 2 mA		BT, 4 mA		OF, 4 mA		OF, 2 mA
Left DBS lead							
Channel 0	−2.01 (0.35)	0.25 (<0.01#)	−2.04 (0.73)	−1.37 (0.10)	0.42 (0.65)	−0.38 (<0.01)	−0.02 (0.24)
Channel 1	−1.49 (0.71)	0.38 (<0.01#)	−3.55 (0.86)	−1.00 (0.10)	0.20 (0.39)	−0.30 (<0.01#)	0.40 (0.42)
Channel 3	−1.28 (0.84)	0.26 (<0.01#)	−3.18 (0.91)	−0.95 (0.11)	0.21 (0.24)	−0.40 (<0.01#)	0.28 (0.63)
Right DBS lead							
Channel 8	−2.34 (0.93)	0.35 (<0.01#)	−3.44 (0.95)	−1.82 (0.11)	−0.31 (<0.01)	−0.36 (<0.01)	0.17 (0.11)
Channel 9	−2.73 (0.96)	0.39 (<0.01#)	−4.39 (0.94)	−2.12 (0.10)	−0.50 (0.07)	−0.38 (<0.01#)	0.06 (0.03)
Channel 10	−1.25 (0.81)	0.32 (<0.01#)	−1.68 (0.65)	−2.32 (0.09)	−0.28 (0.04)	−0.20 (<0.01#)	−1.58 (0.87)
Channel 11	−1.81 (0.86)	0.38 (<0.01#)	−3.28 (0.87)	−2.03 (0.10)	−0.49 (0.11)	−0.33 (<0.01#)	0.01 (<0.01)
Subject 3 (Channel 2 as a reference, Fig. 2I)							
	BT, 4 mA		**BT, 2 mA**		**OF, 2 mA**		**OF, 4 mA**
Left DBS lead							
Channel 0	−5.20 (0.91)	0.56 (<0.01)	−2.75 (0.80)	0.08 (0.02)	1.86 (<0.01)	0.35 (0.03)	0.89 (0.10)
Channel 1	−0.47 (0.82)	0.03 (<0.01)	−0.15 (0.67)	0.05 (0.03)	0.26 (0.52)	0.01 (0.05)	0.24 (0.53)
Channel 3	−0.51 (0.74)	0.03 (<0.01#)	−0.15 (0.31)	0.05 (0.03)	−0.00 (0.24)	0.08 (0.06)	−0.11 (0.10)
Right DBS lead							
Channel 8	−10.75 (0.98)	0.38 (<0.01)	−5.51 (0.97)	−0.20 (0.10)	0.53 (0.79)	−0.25 (0.02)	1.27 (0.94)
Channel 9	−11.09 (0.99)	0.39 (<0.01)	−5.52 (0.97)	−0.28 (0.04)	0.35 (0.66)	−0.19 (0.02)	1.15 (0.93)
Channel 10	−11.47 (0.99)	0.48 (0.01)	−5.65 (0.97)	−0.21 (0.03)	0.33 (0.62)	−0.22 (0.01)	1.02 (0.95)
Channel 11	−11.44 (0.99)	0.50 (0.01)	−5.63 (0.97)	−0.20 (0.06)	0.36 (0.67)	−0.19 (<0.01)	1.02 (0.96)

Each cell shows voltage change values in mV (R^2 value). #p-value for R^2 is not <0.05.
BT: Bitemporal montage; OF: Occipitofrontal montage.

signal, the recording setup high-pass filters the recorded signals with a cut-off of 0.5 Hz or higher. Such a high-pass filter removes the DC or 0 Hz signal, therefore minimizing the bias. However, tDCS is a DC signal with a flat "waveform" making it filter through the traditional recording setup. Therefore, it is challenging to observe voltage changes that are the direct result of or that strongly correlate with tDCS. We overcame this difficulty by not using high-pass filtering, at the compromise of relatively poor fidelity or resolution at a higher frequency range that a typical electrophysiological system may offer. Since we aimed to record tDCS-generated voltage changes using DBS macroelectrodes, and not high frequency neural activity, it was a reasonable trade-off.

Our findings also suggest that tDCS results in an intracerebral passage of currents proportional to the current level. The crude estimate of generated electric field with 4 mA bitemporal tDCS at the level of subthalamic nuclei was 0.19–0.26 mV/mm (Subject 2, channel 9: 4.39 mV ÷ 2.36 cm inter-lead spacing = 1.86 mV/cm; Subject 3, channel 10: 11.47 mV ÷ 4.35 cm inter-lead spacing = 2.63 mV/cm; Tables 2 and 3). Likewise, the crude estimate of the generated electric field with 2 mA bitemporal tDCS was 0.12–0.13 mV/mm. These values are less than 1 mV/mm as recently suggested to be a field strength to have a direct neuromodulatory effect [7]. However, we note that the 1 mV/mm is based on rodent cortex patch clamp recordings *in vivo*, through a skull window, which may not be representative of human anatomy/physiology.

Fig. 2. Voltage change across DBS electrodes change linearly to tDCS dose and is montage specific. **(A)** Schematic diagram of bitemporal tDCS montage: Anode is positioned on the left temporal region and cathode is positioned on the right temporal region. tDCS current flows in a general direction from left to right (red arrow); **(B)** Schematic diagram of occipitofrontal tDCS montage: Anode is positioned on the inion and cathode is positioned on the middle of the forehead. tDCS current flows in a general direction from posterior to anterior (red arrow); **(C–E)** Subject 1 implanted with single 4-channel DBS lead in the left ventrointermediate nucleus (VIM) with lead marked with white arrow on axial section of the MRI (**C**). The subject underwent 2 mA of bitemporal tDCS. When chest reference was used (**D**), all four channels/electrodes/contact points detected about 4 mV of voltage (green traces, color coded to the electrode contact points as shown) that coincide to the ramp-up, plateau and ramp-down of tDCS current (blue trace), but not when channel 2 was used as a reference (**E**). Measured body resistance through tDCS pads was ~4 kΩ that slowly decreased over time in the plateau phase of tDCS and then increased again as tDCS current ramped down (orange trace); **(F–I)** Subject 2 (**F, G**) and 3 (**H, I**) with bilateral implantation of 4-channel DBS leads in subthalamic nucleus (STN, **F**) and internal globus pallidus (GPi, **H**), respectively, show dose-dependent changes in voltage change with tDCS application in bitemporal montage, but not in the occipitofrontal montage. Interindividual variability in tDCS-generated voltage changes (compare **G** to **I**) can be explained by inter-electrode distance (2.36 cm for Subject 2 versus 4.35 cm for Subject 3 – see Table 2). Also, body resistance is lower with 4 mA tDCS application when compared with 2 mA tDCS application irrespective of montage (orange traces, with gray dashed line for comparison). All traces were segment-wise detrended to minimize any DC bias and DC slew artifact. Slow cortical potentials are still apparent in traces even after detrending. Channel numbers on DBS leads follow Medtronic convention. The start and end of tDCS application is marked with magenta and yellow lines, respectively, that span through injected tDCS current (blue) and DBS lead voltage measurements. (For interpretation of the references to color in this figure legend, the reader is referred to the Web version of this article.)

Additionally, pyramidal cells of the cortex typically remain silent unlike neurons on subthalamic nuclei which have a regular firing pattern irrespective of movements [8] and can be more susceptible to even milder strengths of electric fields.

Our experimental protocol ensured that our findings of voltage changes across DBS electrodes were not artifactual. First, tDCS created polarization of the head with reference to the rest of the body. Regarding the reference electrode on the chest wall, intracerebral DBS electrodes did show polarization (Fig. 2C). However, because of the similar distance of all 4 electrodes on a given DBS lead from the anode/cathode, it is unlikely to observe significant voltage difference between them (voltage traces of a given hue – red or green – but the different contrast in Fig. 2C–F). Second, the voltage traces from DBS electrodes are not artifacts resulting from the current "shorting" through the recording setup. Additionally, there is no "cross-talk" across DBS electrode recording channels. Voltage recording is unique from each DBS electrode as there is no duplication of voltage traces across other DBS electrodes. Additionally, several DBS electrode channels showed activity independent of the tDCS stimulation pattern that can be attributed to slow cortical potentials, or activity at the deep nuclei where each particular electrode is situated.

High tDCS amperage leads to reduced body resistance to electricity

Similar to previous tDCS studies [9,10], we found that body or scalp resistance decreases over the ramp-up part of tDCS stimulation and again increases over the ramp-down part of tDCS stimulation. In addition, we found that higher tDCS current can lead to decreased body resistance. This is consistent with an early report of conducting properties of the human skin to direct current [11], and is also consistent with the large electroconvulsive therapy (ECT) literature where resistance drops as soon as the current is applied [12,13]. Body resistance with 4 mA was found to be lower than 2 mA regardless of the order of application. Intra-individual variability is not likely to contribute to the changes in body resistance as the measurements were performed at 2 mA or 4 mA level within several minutes.

Factors affecting the magnitude of voltage changes

Voltage change across a given pair of DBS electrodes is a spatial integration of the EF that ends at the contact points of these electrodes. Therefore, factors affecting the EF will be reflected in the voltage change readings, and are discussed below.

Body resistance and tDCS current

As per Ohm's law (V=IR), applied tDCS current linearly correlates with the generated EF (reflected as voltage change) *only if* the body resistance (R) remains constant. However, in our study, body resistance changes as current amplitude changes (see gray dashed lines comparing resistance in Fig. 2G, I). This suggests that non-linearities may be involved in the tDCS-generated EF. Inter-individual variability in body resistance does exist, and it depends on the skin resistance [14], head dimensions, montage and injected current. Changes in body resistance are unlikely to result in heating of electrodes, as we have previously shown that current up to 4 mA does not lead to significant change in skin temperature under the tDCS electrodes [9]. Head dimensions and tDCS montage have been considered in the modeling of tDCS-generated EFs using FEA techniques [3,15,16]; however, variability in skin resistance and the injected current have never been factored into the determination of the intracerebral EF. Our findings of dose-dependent changes in body resistance echo prior reports [17], and we propose that modeling approaches need to take tDCS dose-dependent resistance values into account when estimating the intracerebral EF.

tDCS montage and DBS lead positioning

The relative orientation of DBS lead(s) to the general vector of current flow determines the detection of the EF and resultant voltage change across the electrode pair. The DBS lead was within the tDCS-generated EF (the recording against percutaneous chest reference showed voltage changes, Fig. 2D). However, we could not detect a dramatic differential voltage across any pair of electrodes on the same DBS lead, possibly because of the near-orthogonal orientation of the DBS lead to the EF (Fig. 2E, G, I, traces of the same color, but different contrast). Similarly, the small differential voltage was detected on electrode pairs under occipitofrontal montage (the vector connecting two leads is near-orthogonal to the overall EF vector, red traces, right half of Fig. 2G, I). However, in the same subject, bitemporal montage showed voltage changes that correlate closely to the tDCS ramp-up, plateau and ramp-down phases (the vector connecting two leads is near-parallel to the overall EF vector, red traces, left half of Fig. 2G, I). The magnitude of these voltage changes appeared to correlate with the distance between the two leads, which explains lower values for Subject 2 (inter-lead distance 2.36 cm at tips) when compared to Subject 3 (inter-lead distance 4.35 cm at tips).

Limitations

This study has several limitations. Only three subjects were tested. There is a lack of multiple repetitions at the given current as we attempted not to deviate from the clinical protocol to minimize the risk to patients. Lack of modeling due to a small number of subjects is another major limitation; however, we will be working on modeling as we collect data from more subjects.

Summary

This report offers direct evidence that tDCS (applied through the scalp) can generate EF deep inside the brain, in contrast to the perception that tDCS currents may not penetrate beyond the cortex. It has several implications for future tDCS research: First, it suggests that the EF vectors are montage-dependent, emphasizing the importance of proper electrode positioning or montage tailored to a specific disease condition. Second, although it is unclear whether the detected EF at the subcortical level is adequate to incur physiological or behavioral responses, it is reasonable to include and examine these subcortical regions in future investigations of tDCS-modulated neural networks. Third, our finding of dose-dependent changes in body resistance suggests that future modeling approaches need to account for tDCS dose-dependent resistance values when estimating intracerebral EFs. Finally, our findings *qualitatively, not yet quantitatively,* corroborate the predictions of EF from the existing tDCS computational models. These *in vivo* human recordings can, in turn, quantitatively refine and optimize these tDCS models once more data is collected.

Acknowledgments

Authors thank Mr. Gregory Leichner (Medtronic, Inc., Minneapolis, MN) for his generous support of the experimental hardware setup.

Appendix A. Supplementary data

Supplementary data related to this article can be found at https://doi.org/10.1016/j.brs.2018.03.006.

Conflicts of interest

Dr. Marom Bikson is a stakeholder in Soterix Medical, Inc.

Funding

This project was funded by National Center of Neuromodulation for Rehabilitation (P2CHD086844). PYC, SAK, MSG, and WF acknowledge grant support from an Institutional Development Award from the National Institute of General Medical Sciences of the National Institutes of Health (P20GM109040). PYC acknowledges fellowship grant support from SC-CoAST/NIH StrokeNet (U10NS086490) and American Heart Association (15SFDRN24480016). GJR acknowledges grant support from National Institute of Health (K23NS091391). SAK acknowledges grant support from the Rehabilitation Research and Development Service (I01RX001935) of the VA. MB acknowledges grant support from National Institute of Mental Health (R01MH111896) and National Institute of Neurological Disorders and Stroke (R01NS101362). WF acknowledges grant support from American Heart Association (14SDG1829003).

References

[1] Lefaucheur J-P, Antal A, Ayache SS, Benninger DH, Brunelin J, Cogiamanian F, et al. Evidence-based guidelines on the therapeutic use of transcranial direct current stimulation (tDCS). Clin Neurophysiol 2017;128:56–92.
[2] Underwood E. NEUROSCIENCE. Cadaver study challenges brain stimulation methods. Science 2016;352:397.
[3] Datta A, Bansal V, Diaz J, Patel J, Reato D, Bikson M. Gyri-precise head model of transcranial direct current stimulation: improved spatial focality using a ring electrode versus conventional rectangular pad. Brain Stimulation 2009;2:201–7. e1.
[4] Opitz A, Falchier A, Yan CG, Yeagle EM, Linn GS, Megevand P, et al. Spatiotemporal structure of intracranial electric fields induced by transcranial electric stimulation in humans and nonhuman primates. Sci Rep 2016;6:31236.
[5] Huang Y, Liu AA, Lafon B, Friedman D, Dayan M, Wang X, et al. Measurements and models of electric fields in the in vivo human brain during transcranial electric stimulation. Elife 2017;6.
[6] Ruhnau P, Rufener KS, Heinze HJ, Zaehle T. Sailing in a sea of disbelief: in vivo measurements of transcranial electric stimulation in human subcortical structures. Brain Stimul 2018;11(1):241–3.
[7] Voroslakos M, Takeuchi Y, Brinyiczki K, Zombori T, Oliva A, Fernandez-Ruiz A, et al. Direct effects of transcranial electric stimulation on brain circuits in rats and humans. Nat Commun 2018;9:483.
[8] Wilson CJ. Oscillators and oscillations in the basal ganglia. Neuroscientist 2015;21(5):530–9.
[9] Chhatbar PY, Chen R, Deardorff R, Dellenbach B, Kautz SA, George MS, et al. Safety and tolerability of transcranial direct current stimulation to stroke patients - a phase I current escalation study. Brain Stimul 2017;10:553–9.
[10] Hahn C, Rice J, Macuff S, Minhas P, Rahman A, Bikson M. Methods for extra-low voltage transcranial direct current stimulation: current and time dependent impedance decreases. Clin Neurophysiol 2013;124:551–6.
[11] Rosendal T. Studies on the conducting properties of the human skin to direct current. Acta Physiol 1943;5:130–51.
[12] Sackeim HA. Physical properties of the ECT stimulus. J ECT 1994;10:140–52.
[13] Sackeim HA, Long J, Luber B, Moeller JR, Prohovnik I, Devanand DP, et al. Physical properties and quantification of the ECT stimulus: I. Basic principles. Convuls Ther 1994;10:93–123.
[14] Andersen KE, Maibach HI. Black and white human skin differences. J Am Acad Dermatol 1979;1:276–82.
[15] Lee W, Seo H, Kim S, Cho M, Lee S, Kim T-S. Influence of white matter anisotropy on the effects of transcranial direct current stimulation: a finite element study. In: 13th international conference on biomedical engineering. Springer; 2009. p. 460–4.
[16] Suh HS, Kim SH, Lee WH, Kim TS. Realistic simulation of transcranial direct current stimulation via 3-d high-resolution finite element analysis: effect of tissue anisotropy. Conf Proc IEEE Eng Med Biol Soc 2009;2009:638–41.
[17] Stephens WGS. The current-voltage relationship in human skin. Med Electron Biol Eng 1963;1:389–99.